Langmuir
Article
pubs.acs.org/Langmuir

Shaping Gold Nanocomposites with Tunable Optical Properties

Manuel A. Martins,[†] Sara Fateixa,[†] Ana V. Girão,[†] Sérgio S. Pereira,[‡] and Tito Trindade*[,†]

[†]*Chemistry Department and CICECO, University of Aveiro, 3810-193 Aveiro, Portugal, and* [‡]*CICECO, University of Aveiro, 3810-193 Aveiro, Portugal*

Received March 3, 2010. Revised Manuscript Received April 13, 2010

We report the synthesis of morphological uniform composites using miniemulsions of poly(*tert*-butyl acrylate) or poly(styrene) containing organically capped gold nanocrystals (NCs). The optical features of such hybrid structures are dominated by plasmonic effects and depend critically on the morphology of the resulting nanocomposite. In particular, we demonstrate the ability to tune the overall optical response in the visible spectral region by varying the Au NCs arrangement within the polymer matrix, and therefore the interparticle plasmon coupling, using Au NCs resulting from the same batch of synthesis. This is a consequence of two well-known effects on the optical properties of Au particles: the variation of the surrounding dielectric refractive index and interparticle plasmonic coupling. The research reported here shows a general strategy to produce optical responsive nanocomposites via control of the morphology of submicrometric polymer particles containing metal nanocrystals and thus is an alternative to the more common strategy of size tuning metal nanoparticles used as nanofillers.

Introduction

The use of colloidal gold can be traced back to the fifth century B.C. in Egypt and China and since then there are several examples of its decorative and medicinal properties.[1] Nowadays, gold colloids in all their diversity occupy a prominent place in nanotechnology due to their unique optical, electronic, chemical, and magnetic properties that have been exploited in diverse applications.[2,3] Since the pioneering studies of Michael Faraday on gold hydrosols, it is known that gold shows optical properties strongly dependent upon particle size.[4] Later studies formulated by Mie allowed the resolution of the Maxwell equations for the absorption and scattering of electromagnetic radiation by small spheres in dielectrics.[5] Since then, a myriad of gold nanostructures with variable morphological characteristics have been reported in which the optical absorption can be fine-tuned.[6−10] This optical tuning is a result of changes in the so-called surface plasmon resonance (SPR), i.e., the frequency at which conduction electrons oscillate in response to the alternating electrical field of incident electromagnetic radiation.[11] The oscillation modes are characterized by a strong field enhancement at the interface, while the electric field vector decays exponentially away from the surface, leading to a small penetration depth into the metal. When the dimensions of the metal are reduced, boundary and surface effects become very important, and therefore the optical properties of small nanoparticles are dominated by such a collective oscillation of conduction electrons in resonance with the incident electromagnetic radiation.[12,13] The spectral position, damping, and strength of the dipole as well as the higher-order plasmon resonances of Au nanoparticles all depend on size and shape.[7,10,14,15] The optical response of Au NCs also depends on other parameters, such as the dielectric function of the surrounding medium[16−19] and the distance between neighboring NCs,[20−22] which in turn determine interparticle plasmon coupling. The judicious variation of these parameters allows the optical properties of Au nanostructures to be tailored.

Functional polymer/nanoparticle composites show properties that arise from the inorganic component, conjugated to physical and chemical properties of the polymer matrix, which allows for example mild temperature processing and tunable mechanical behavior. In addition, the arrangement of the inorganic nanofillers in the organic matrix might originate new collective properties. In this regards several polymer nanocomposites containing metals, metal oxides or sulfides, have been reported in recent literature. Examples can be found in recent reviews, including methodologies for *in situ* synthesis of metal nanoparticles in polymer matrices,[23] fabrication of optically active nanocomposites,[24] the use of functional inorganic nanoparticles in transparent polymers,[25] fundamental aspects on manufacturing and

*Corresponding author. E-mail: tito@ua.pt.

(1) Ghosh, S. K.; Pal, T. *Chem. Rev.* **2007**, *107*, 4797–4862.
(2) Daniel, M.; Astruc, D. *Chem. Rev.* **2004**, *104*, 293–346.
(3) Wang, Z.; Ma, L. *Coord. Chem. Rev.* **2009**, *253*, 1607–1618.
(4) Faraday, M. *Philos. Trans. R. Soc. London* **1857**, 147.
(5) Mie, G. *Ann. Phys.* **1908**, *25*, 377.
(6) Grzelczak, M.; Pérez-Juste, J.; Mulvaney, P.; Liz-Marzán, L. M. *Chem. Soc. Rev.* **2008**, *37*, 1783–1791.
(7) Link, S.; El-Sayed, M. A. *J. Phys. Chem. B* **1999**, *103*, 8410–8426.
(8) Wang, H.; Wu, Y.; Lassiter, B.; Nehl, C. L.; Hafner, J. H.; Nordlander, P.; Halas, N. J. *Proc. Natl. Acad. Sci. U.S.A.* **2006**, *103*, 10856–10860.
(9) Hu, M.; Chen, J.; Li, Z.; Au, L.; Hartland, G. V.; Li, X.; Marquez, M.; Xia, Y. *Chem. Soc. Rev.* **2006**, *35*, 1084–1094.
(10) Njoki, P. N.; Lim, I. S.; Mott, D.; Park, H.; Khan, B.; Mishra, S.; Sujakumar, R.; Luo, J.; Zhong, C. *J. Phys. Chem. C* **2007**, *111*, 14664–14669.
(11) Liz-Marzán, L. M. *Mater. Today* **2004**, 26–31.
(12) Mulvaney, P. *Langmuir* **1996**, *12*, 788–800.
(13) Liz-Marzán, L. M. *Langmuir* **2006**, *22*, 32–41.
(14) Jain, P. K.; Lee, K. S.; El-Sayed, I. H.; El-Sayed, M. A. *J. Phys. Chem. B* **2006**, *110*, 7238–7248.
(15) Pérez-Juste, J.; Pastoriza-santos, I.; Liz-Marzán, L. M.; Mulvaney, P. *Coord. Chem. Rev.* **2005**, *249*, 1870–1901.
(16) Jiang, G.; Baba, A.; Ikarashi, H.; Xu, R.; Locklin, J.; Kashif, K. R.; Shinbo, K.; Kato, K.; Kaneko, F.; Advincula, R. *J. Phys. Chem. C* **2007**, *111*, 18687–18694.
(17) Liz-Marzán, L. M.; Giersig, M.; Mulvaney, P. *Langmuir* **1996**, *12*, 4329–4335.
(18) Kelly, K. L.; Coronado, E.; Zhao, L. L.; Schatz, G. C. *J. Phys. Chem. B* **2003**, *107*, 668–677.
(19) Underwood, S.; Mulvaney, P. *Langmuir* **1994**, *10*, 3427–3430.
(20) Ung, T.; Liz-Marzán, L. M.; Mulvaney, P. *Colloids Surf., A* **2002**, *202*, 119–126.
(21) Wei, Q.; Su, K.; Durant, S.; Zhang, X. *Nano Lett.* **2004**, *4*, 1067–1071.
(22) Jain, P. K.; Qian, W.; El-Sayed, M. A. *J. Phys. Chem. B* **2006**, *110*, 136–142.
(23) Ramesh, G. V.; Porel, S.; Radhakrishnan, T. P. *Chem. Soc. Rev.* **2009**, *38*, 2646–2656.
(24) Caseri, W. *Chem. Eng. Commun.* **2009**, *196*, 549–572.
(25) Althues, H.; Henle, J.; Kaskel, S. *Chem. Soc. Rev.* **2007**, *36*, 1454–1465.

processing of polymer nanocomposites,[26] and diverse chemical approaches to obtain magnetic, electronically active, and stimuli-responsive nanocomposites.[27−29]

Although a variety of papers describing optical effects arising from morphological control of gold nanostructures have been reported, there is great interest to develop new platforms envisaging the fabrication of devices.[2] For example, recently we have shown a method to integrate colloidal gold NCs into optically active III/V nitride heterostructures, i.e., InGaN/GaN multiple quantum wells that are the basis of efficient light-emitting devices in the visible and UV spectral regions, thus merging *bottom-up* and *top-down* approaches into the fabrication of hybrid functional nanostructures.[30] The association of soft materials, such as low-temperature processed polymers and gold nanostructures, constitutes a step forward in the miniaturization of devices. The present investigation shows that it is possible to tune the surface plasmon energy of gold nanostructures by changing the morphology of submicrometer composite structures containing that metal. This is demonstrated by incorporating Au NCs resulting from the same synthesis batch in polymer matrices obtained in different reaction conditions.

Experimental Section

Chemicals. The following chemicals were used as purchased: $HAuCl_4 \cdot 3H_2O$ (Sigma-Aldrich, 99.9%), ethylene glycol (EG, Aldrich, 99%), oleylamine (OA, Aldrich, 70%), trioctylamine (TOA, Aldrich, 98%), $NaHCO_3$ (Panreac, 99%), trioctylphosphine oxide (TOPO, Fluka, 97%), potassium persulfate (KPS, Panreac, 98%), dodecyl sulfate sodium salt (SDS, Aldrich, 98%), hexadecane (HD, Aldrich, 99%), tetrahydrofuran (THF, Panreac, 99.5%). The monomers, *tert*-butyl acrylate (*t*BA) and styrene (ST), were purified over a column of neutral aluminum oxide and stored at 4 °C. Water was purified using a Sation 8000/Sation 9000 purification unit.

Synthesis of Organically Capped Au Nanoparticles. Organically capped gold nanoparticles were prepared using a modification of the polyol method described by Fievet et al.[31,32] A solution containing $HAuCl_4 \cdot 3H_2O$ (0.15 M) in ethylene glycol (10 mL) was injected into a hot solution containing 30 mL of trioctylamine and 10 mL of oleylamine (120 °C) for 30 min, under a nitrogen stream. As the reaction took place, the initial yellow solution turned to dark red. After cooling to room temperature, the formation of two phases was observed: the top one, with dark red color, rich in gold nanoparticles, and the bottom one, a clear solution consisting mainly of ethylene glycol. The nanoparticles were washed with 2-propanol and methanol and isolated by centrifugation (at 3000 or 6000 rpm). The nanoparticles were then dispersed in toluene, and the procedure was repeated twice to remove the excess of capping agent (TOA and OA). In order to obtain TOPO capped Au NCs, the nanoparticles described above were injected into 50 mL of TOPO at 120 °C, for 4 h, to exchange the surface TOA/OA molecules by TOPO. The TOPO-capped Au NCs were then washed with methanol and isolated by centrifugation (6000 rpm).

Synthesis of Gold/Polymer Nanocomposites. For the *in situ* polymerizations in miniemulsion, the procedure was as follows. For a 25 mL batch, the organically capped Au NCs were homogeneously mixed with *t*BA or ST (0.032 mol) and hexadecane (3.31×10^{-4} mol) to form a stable dispersion. This mixture was then mixed in an aqueous solution of dodecyl sulfate sodium salt (SDS, 2×10^{-4} mol) and $NaHCO_3$ (9.81×10^{-4} mol) and was kept under vigorous stirring over 30 min, followed by sonication (amplitude 80%, 20 W power, Sonics-Vibracel Sonifier) for 7 min. The miniemulsion obtained was transferred to a conventional "jacket" glass reactor (30 mL capacity), equipped with a thermostatic bath, mechanical stirrer, and nitrogen inlet. After purging with N_2, the temperature of the miniemulsion was set to 70 ± 1 °C, and aqueous potassium persulfate (KPS, 6.78×10^{-5} mol) was added to the reaction, thus setting the zero time for the polymerization. The reaction took place over 4 h under mechanical stirring at 500 rpm. Monomer conversion was gravimetrically evaluated, and typical values of 90% have been achieved.

Instrumentation. A Jasco V 560 UV/vis spectrophotometer was used for recording the UV/vis absorption spectra of the colloids and the diffuse reflectance spectra of the nanocomposite powders; the latter were converted to Kubelka−Munk units. The infrared spectra were recorded using a Matson 700 FTIR spectrometer. Dynamic light scattering (DLS) measurements were recorded using a Malvern Zetasizer Nano ZS using water or toluene as a solvent to dilute the samples. The measurements were recorded at 25 °C using quartz cells. X-ray powder diffraction (XRD) was performed on samples deposited on silicon substrates, using a Philips X'Pert instrument operating with Cu Kα radiation (λ = 1.541 78 Å) at 40 kV/50 mA. Transmission electron microscopy (TEM) was carried out on a Hitachi H-9000 microscope operating at 300 and 200 kV. To prepare the TEM samples, a drop of the diluted colloid was deposited on a carbon-coated copper grid, and the solvent was left to evaporate. Scanning electron microscopy (SEM) images were carried out using a Hitachi SU-70 and EDX mapping was performed using an EDX Bruker Quantax 400. Gold content in the nanocomposites was measured by ICP using a Jobin-Yvon JY70Plus spectrometer.

Results and Discussion

In order to obtain organically capped gold nanocrystals (NCs), $HAuCl_4$ was reduced at 120 °C in the presence of ethylene glycol, which acts both as a solvent and as a reducing agent. It is well-known that reduction of metal salts in liquid polyols occurs through the oxidation of an acetaldehyde to a diacetyl, produced by the dehydration of the ethylene glycol at high temperature.[31,32] In this work, the polyol method was slightly adapted by preparing an ethylene glycol reacting mixture that was then injected into TOA/OA at 120 °C. This mixture of organic solvents allows a steady growth of the metal seeds generated after injection of the reactants, thus leading to NCs with controlled morphology, as those shown in Figure 1. In this case, the average diameter (and standard deviation) as determined by DLS was 6.9 ± 1.1 nm for Au NCs in the colloid as compared to 5.1 ± 1.1 nm for Au NCs dispersed in a Cu grid and then analyzed by TEM. The average diameters are close to each other within the indicated error limits, and the small discrepancy is because DLS measures the hydrodynamic radius that takes into account the NCs outer shell composed of long alkyl chain coordinating molecules (TOA/OA). In fact, using the synthetic procedure as described above, the Au NCs became coated with TOA/OA molecules that not only prevent the NCs coalescence but also turn the Au NCs dispersible in nonpolar solvents. This also allows the exchange of TOA/OA molecules by other organic capping molecules without compromising the morphological integrity of the metal cores. For example, on the basis of TEM analysis, we concluded that the as-prepared Au NCs did not exhibit significant morphological differences after being treated with TOPO; in this case the average diameter of the NCs was 5.9 ± 0.9 nm as obtained from analysis of the TEM images.

Further evidence for the presence of the organic capping at the nanoparticles surfaces was obtained by FT-IR spectroscopy of

(26) Hussain, F.; Hojjati, M.; Okamoto, M.; Gorga, R. E. *J. Compos. Mater.* **2006**, *40*, 1511–1575.
(27) Pyun, J. *Polym. Rev.* **2007**, *47*, 231–263.
(28) Sudeep, P. K.; Emrick, T. *Polym. Rev.* **2007**, *47*, 155–163.
(29) Schmidt, A. *Colloid Polym. Sci.* **2007**, *285*, 953–966.
(30) Pereira, S. M.; Martins, M. A.; Trindade, T.; Watson, I. M.; Zhu, D.; Humphreys, C. J. *Adv. Mater.* **2008**, *20*, 1038–1043.
(31) Fievet, F.; Lagier, J. P.; Blin, B.; Beaudoin, B.; Figlarz, M. *Solid State Ionics* **1989**, *32−3*, 198–205.
(32) Fievet, F.; Lagier, J. P.; Figlarz, M. *MRS Bull.* **1989**, *14*, 12.

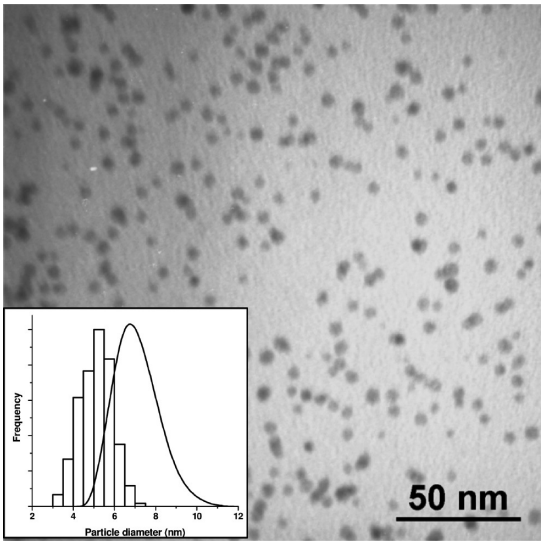

Figure 1. Transmission electron microscopy (TEM) image of Au nanocrystals prepared by the polyol method in the presence of TOA/OA. Inset shows the respective particle size histogram: TEM size distribution bars and DLS size distribution line.

powders composed of Au NCs and thoroughly washed after the synthesis (see Supporting Information). As discussed above, the OA/TOA molecules coating the Au NCs render these particles surface hydrophobic, thus compatible with *tert*-butyl acrylate (*t*BA) and styrene monomers. A miniemulsion polymerization in the presence of the Au NCs was then used to perform the polymer encapsulation, as detailed in the Experimental Section.

A first evidence of the presence of Au NCs in the polymer nanocomposite was the purple color observed in the final aqueous emulsion, further confirmed by a band centered at 543 nm in the visible spectrum of pure Au/P*t*BA nanocomposites (Figure 2). When compared to the original Au/TOA/OA NCs (red color), this band is broader and is slightly shifted to longer wavelengths ($\Delta\lambda$ = 28 nm). This band broadening extending to longer wavelength explains the purple color observed for the Au/P*t*BA emulsion when compared to the original red Au colloid (Figure 2). The chemical composition of the Au/P*t*BA nanocomposite was confirmed by powder XRD and FT-IR spectroscopy. Thus, XRD peaks corresponding to the most intense peaks of face centered cubic Au were observed at 2θ 38.3° (111) and 44.6° (200) (see Supporting Information). Note that at lower diffraction angles the peaks attributed to the polymer matrix appear as more intense due to the relative small amount of Au NCs present in the composite (typically 2% w/w). As expected, the FT-IR spectrum of the Au/P*t*BA nanocomposite was found to be very similar to that of pure P*t*BA, here used as matrix (see Supporting Information).

Figure 3 shows TEM images of Au/P*t*BA nanocomposites obtained as described above. The nanocomposite particles appear as spheres whose dimensions are typically in the 300−500 nm range. The dark contrast observed in these composite nanoparticles indicates that each bead is composed of a large number of Au NCs homogeneously wrapped by polymer chains, as detailed in Figure 3 (right). The Au NCs dispersion within each composite particle was unequivocally confirmed by SEM and EDX mapping of these samples (Figure 4).

Although polymer encapsulation of inorganic nanoparticles using miniemulsion polymerization techniques has been previously

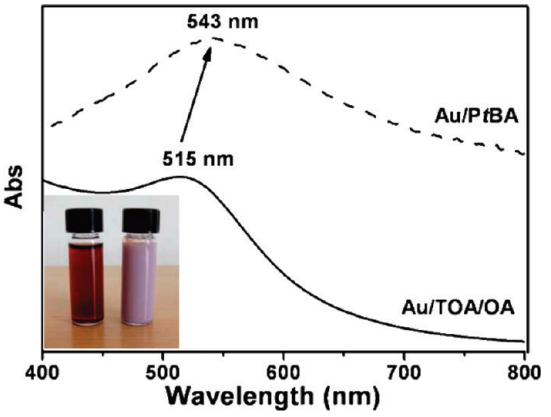

Figure 2. Visible spectra of Au/P*t*BA nanocomposites powders and of the original Au colloid. The inset shows micrographs of the Au toluene colloid (red) and the Au/P*t*BA emulsion (purple).

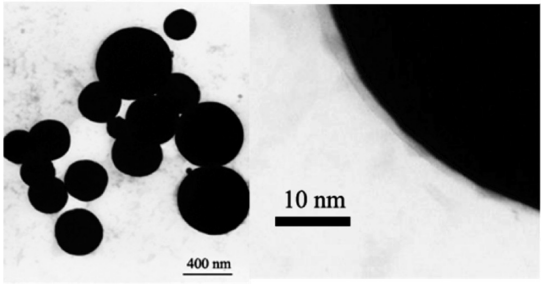

Figure 3. TEM images of Au/P*t*BA nanocomposite beads.

reported for organically capped quantum dots and magnetic nanoparticles,[33−35] the present system seems particularly interesting because each composite particle can be high loaded with nanofillers. Size NCs concentration and the nature of the capping ligands are parameters that influence the polymer encapsulation. It is evident from our work that during the miniemulsion polymerization, the Au NCs tend to ensemble inside the growing polymer beads of P*t*BA. In the case of the Au−P*t*BA composites, the Au NCs seem to be homogeneously distributed along the composite volume as it can be observed from the microscope images of longitudinal cuts of the polymer composite particles (see Supporting Information). Moreover, EDX measurements (Figure 4) performed on this sample along a line scan passing roughly through the meridian of the composite sphere show an increase of gold content across the particle composite volume which is compatible with an homogeneous distribution of gold NPs inside the polymer bead in opposition to a core/shell type structure.

We note here that the above results do not allow distinguishing between irreversible agglomerated Au NCs inside the polymer beads from individualized single Au NCs wrapped by polymer chains. In this respect, it is instructive to compare the optical spectra of both the original Au colloid and of the Au NCs dispersed in the composite sample. Therefore, the latter sample was selectively analyzed by UV/vis spectroscopy and TEM, after dissolving the Au nanocomposite in tetrahydrofuran (THF). The THF dissolved the polymer chains destroying the latex structure, but the Au NCs remained intact in solution. Figure 5 shows the UV/vis spectra for the Au colloid previous the polymerization and

(33) Esteves, A. C.; Barros-Timmons, A. M.; Monteiro, T.; Trindade, T. *J. Nanosci. Nanotechnol.* **2005**, *5*, 766–771.

(34) Martins, M. A.; Neves, M. C.; Esteves, A. C.; Girginova, P. I.; Guiomar, A. J.; Amaral, V. S.; Trindade, T. *Nanotechnology* **2007**, *18*, 215609.

(35) Pereira, A. S.; Rauwel, P.; Reis, M. S.; Silva, N. J.; Barros-Timmons, A. M.; Trindade, T. *J. Mater. Chem.* **2008**, *18*, 4572–4578.

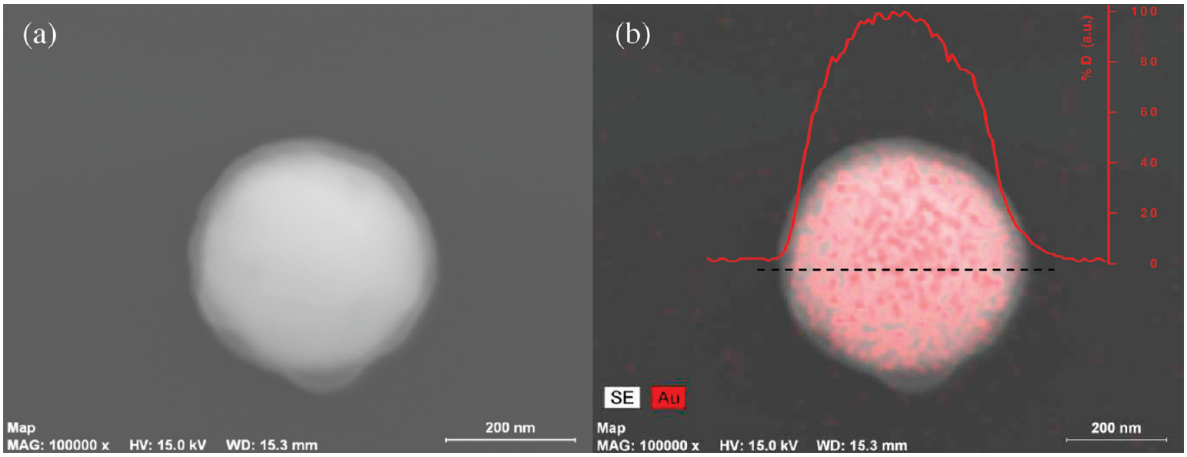

Figure 4. SEM image (a) and EDX mapping (b) of gold NCs (red dots) in Au/P*t*BA nanocomposite beads. Corresponding gold content distribution along the line scan displayed (inset).

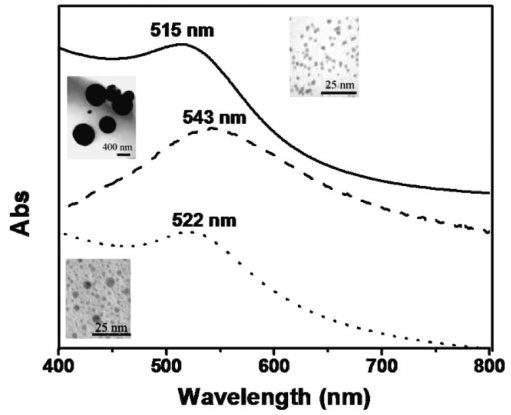

Figure 5. UV−vis spectra and corresponding TEM images of Au NCs (—) and for the Au/P*t*BA nanocomposite before (---) and after treatment with THF (···).

the two Au/P*t*BA nanocomposite samples, before and after treatment with THF. It is clear that the UV/vis spectrum of the nanocomposite treated with THF resembles that one of the original Au colloid, with the SPR band centered at 522 nm. This result is consistent with the presence of intact Au NCs encapsulated in the polymer matrix. It would be also possible that some differences observed in the spectra shown in Figure 5 could be due to the distinct recording mode of the spectra (absorption or reflectance mode); this could be mainly true for the larger scattering observed at longer wavelengths, but it is unlikely to explain the shift in the SPR band. In fact, TEM analysis performed on the sample treated with THF confirmed the presence of monodispersed Au NCs similar to the original gold colloid. A few slightly larger particles were also present which is likely due to exchange reactions that had occurred at the NCs surfaces, leading to Au NCs prone to coalescence during TEM sample preparation.

It is well-known that the refractive index of the surrounding medium as well as the average distance between neighboring Au particles both influence the spectral features of samples containing dispersed Au NCs. Thus, the increase of the refractive index of the medium surrounding the nanoparticles,[20,36] as well as the decrease in the particles interdistance, leads to a red shift of the SPR peak position.[19−21] In principle, optical tuning of Au-containing

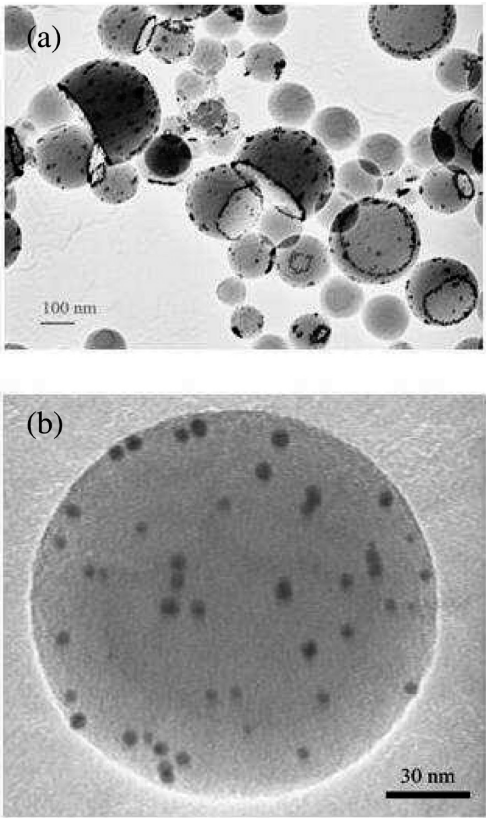

Figure 6. TEM images of polystyrene nanocomposites containing (a) Au/TOA/OA and (b) Au/TOPO.

polymer beads, even if made of Au nanofillers characterized by a specific SPR frequency, could be achieved provided there is access to chemical methods that enable not only to vary the polymer (and thus the matrix refractive index) but also to control the morphology of the final nanocomposite. We note that this approach is distinct, and in fact an alternative, to the more common method that employs already made Au NCs of variable morphology and size. Therefore, this chemical strategy toward optical tuned gold nanocomposites was investigated here.

An interesting property of the Au/P*t*BA nanocomposites reported in this work is the possibility to achieve a high density of Au nanospheres in each single composite particle, thus resulting in a slightly red-shifted SPR band ($\Delta\lambda$ = 28 nm) when

(36) Kang, Y.; Taton, T. A. *Angew. Chem., Int. Ed.* **2005**, *44*, 409–412.

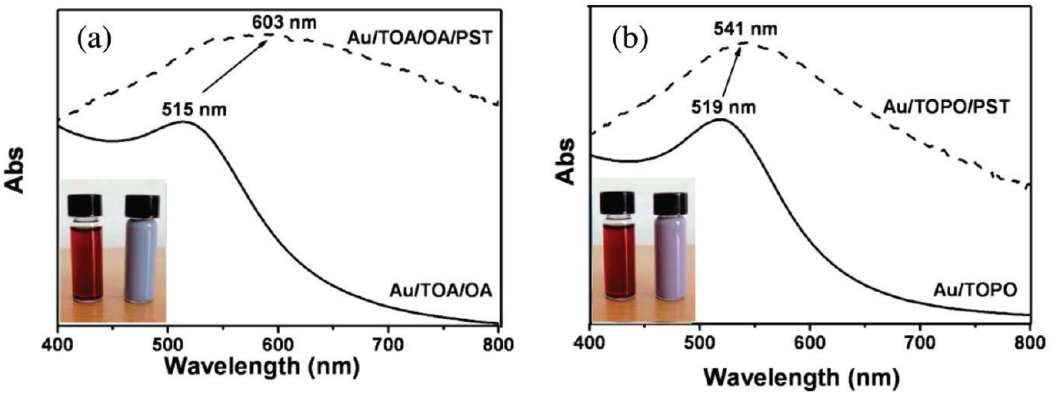

Figure 7. Visible spectra of the Au/PST nanocomposites and of the original Au colloid, obtained from (a) Au/TOA/OA and (b) Au/TOPO nanoparticles. The inset shows micrographs of the Au toluene colloid (red) and the Au/PST emulsions (blue/purple).

compared to the original Au colloid (Figure 2). In order to address these observations, calculations were carried out to simulate the optical spectra of the nanocomposite.[37] First we note that this red shift cannot be assigned to irreversible coalescence of the Au NCs into larger particles as demonstrated before by the regeneration of the initial Au NCs upon THF polymer dissolution. On the other hand, the interparticle distance alone does not account for such a small shift because the dense nanocomposites observed by TEM should exhibit a larger red shift due to the very close proximity between the Au NCs. Normalized visible spectra were calculated for 7 nm Au nanospheres surrounded by a dielectric with distinct refractive indexes (see Supporting Information). It is clear that the variation of the refractive index of the surrounding medium of the Au NCs in the nanocomposites explains, in this case, the shift of the SPR toward longer wavelengths and the extended absorption tail at longer wavelengths.

Significant coupling between the Au NCs within the polymer matrix would be expected for the case of interparticle distances of the order of the particles diameter. Thus, since Figure 2 does not show signs of such effect, the observed optical spectra are consistent with an extensive nanoparticles dispersion within the host matrix, which seems to enforce a particle−particle distance that exceeds the necessary distance for interparticle plasmon coupling. It is likely that mobile polymer chains wrap the Au NCs, hence acting as a dielectric spacer that prevents electrical field coupling between neighboring Au NCs. In this regards, the dependence of the SPR band of Au colloids due to dielectric screening by adsorbed polymers has been recently reported.[38]

The optical properties of Au polymer nanocomposites reported here depend also on the morphology of the resulting nanocomposite, for example, the type of arrangement of the Au NCs within the polymer beads. In this case polystyrene (PST) nanocomposites were prepared, and the dispersion of the Au NCs during the miniemulsion was varied by changing the organic coating at their surfaces. Figure 6 shows the TEM images of two kinds of PST nanocomposites obtained by using Au NCs coated with TOA/OA and TOPO. Although at the moment we cannot anticipate a mechanism that explains the observed morphologies, it seems that interphase phenomena and the relative dispersion of the Au NCs in the monomer are particularly relevant. In particular, we note that the "nano-jelly fish" (Figure 6a) type morphology seems to result from the presence of Au NCs at the nanoreactors interphase during the polymerization. Although the nature of the organic capping seems to influence the arrangement of the Au NCs in the polymer, it is also reasonable to suggest that the distinct morphologies observed might be glass transition (T_g) dependent. The fact that the *in situ* polymerization occurs at a temperature (ca. 70 °C), hence well above the T_g of P*t*BA (43 °C) and below the T_g of PST (117 °C), certainly had an effect on the dispersion of the Au NCs within the polymer chains. In that case the dispersion of Au NCs in the polymer beads would be facilitated in the polymerization of P*t*BA, which is in agreement with the homogeneous distribution of the Au NCs, as observed in Figures 3 and 4.

For the nanocomposites described above the effect of interparticle coupling is evident in the optical spectra (Figure 7a), with the emergence of a broad absorption band extending into the near-infrared region. This correlates well with the presence of Au NCs in a "ring" arrangement with interparticle distances comparable to their diameter, as shown by TEM in Figure 6. Finally, for the case of the PST based nanocomposite (Figure 6b) containing Au/TOPO nanocrystals, a SPR located at a wavelength close to that one observed for the original Au colloid is expected (Figure 7b). This is because the medium refractive index is not much different, and these nanocomposites, unlike the Au/P*t*BA shown above, are less populated in Au NCs.

Conclusions

Synthesis of optically distinct polymer based composites containing Au NCs of the same batch of synthesis has been shown to be viable using a miniemulsion *in situ* polymerization method. The main idea behind this strategy was to produce stable aqueous emulsions of nanocomposite particles whose optical properties depend not only on the Au NCs employed in their synthesis but also on the resulting morphology for the final composites. In this regards, the type of organic capping at the surface of Au NCs seems to play a crucial role in determining the type of arrangement of Au NCs in the polymer matrix during the nanocomposites preparation. Moreover, in light of the distinct morphologies observed for the PST and P*t*BA nanocomposites, the use of polymers with distinct T_g seems also to lead to distinct NCs arrangements during the synthesis of the respective nanocomposite though further research is planned on this topic. In a perspective of materials design, the method described here provides a route to produce a variety of optically tunable Au composites for nanodevices. Moreover, due to their colloidal stability, they seem particularly interesting for *in vitro* clinical diagnostics applications.

(37) MiePlot V4.1. A Computer Program For Scattering Of Light From A Sphere Using Mie Theory & The Debye Series, Philip Laven.
(38) Schneider, G.; Decher, G.; Nerambourg, N.; Praho, R.; Werts, M. H.; Blanchard-Desce, M. *Nano Lett.* **2006**, *6*, 530–536.

Acknowledgment. We thank Fundação para a Ciência e Tecnologia (FCT/FEDER) for the following grants: SFRH/BD/29475/2006 (M. A. Martins), SFRH/BD/66460/2009 (S. Fateixa), SFRH/BPD/66407/2009 (A. V. Girão), and project PTDC/QUI/67712/2006. We thank Professor Ana Barros-Timmons for helpful discussions. Microscopy analysis was supported by RNME-Pole University of Aveiro FCT Project REDE/1509/RME/2005.

Supporting Information Available: FTIR spectra of organically capped gold nanocrystals and gold−polymer nanocomposites; scheme of the miniemulsion polymerization; XRD powder patterns for Au/P*t*BA nanocomposites; SEM image of a longitudinal cut of the Au−P*t*BA composite; calculated visible spectra for Au nanospheres (7 nm). This material is available free of charge via the Internet at http://pubs.acs.org.